ulm university universität
uulm

Fakultät für Naturwissenschaften

Institute of Theoretical Physics

Title of the work

Bachelor Thesis

Submitted by:
Jan Bulling
jan.bulling@uni-ulm.de
1109395

Supervised by:
Marit O. E. Steiner, Julen S. Pedernales, Martin B. Plenio

Abstract

Contents

1 Introduction

1.1 Feynman's Gedankenexperiment

2 A first look at the problem

The quantum aspects of gravity can be tested with entanglement conveyed by gravitational interaction. A possible and naturally arising experiment to observe gravitationally induced entanglement is described in this chapter. The rest of this thesis is about experimental issues with the descried procedure that are present in a real laboratory setting.

The experiment requires the ability to manipulate macroscopic massive bodies quantum mechanically by inducing a cat-state (a macroscopic spatial superposition state) or a squeezed state (!!!!!!!). This can be done in practice by e.g. utilizing a spin coupled to the center-of-mass motion of the object and a magnetic field gradient [1]. In the rest of this thesis I assume that all required states can be prepared. Remarkable progress has been made in this field of quantum optomechanics in the last decade !!!SOURCES FROM E.G. ASPELMAYER!!!!. Levitating the particles in a trap in a vacuum can increase environmental isolation by avoiding contact with surrounding noise. The additional forces due to the trapping can be well studied in advance.

The general problem is illustrated in fig. 2.1. Two bodies with masses M_A and M_B are

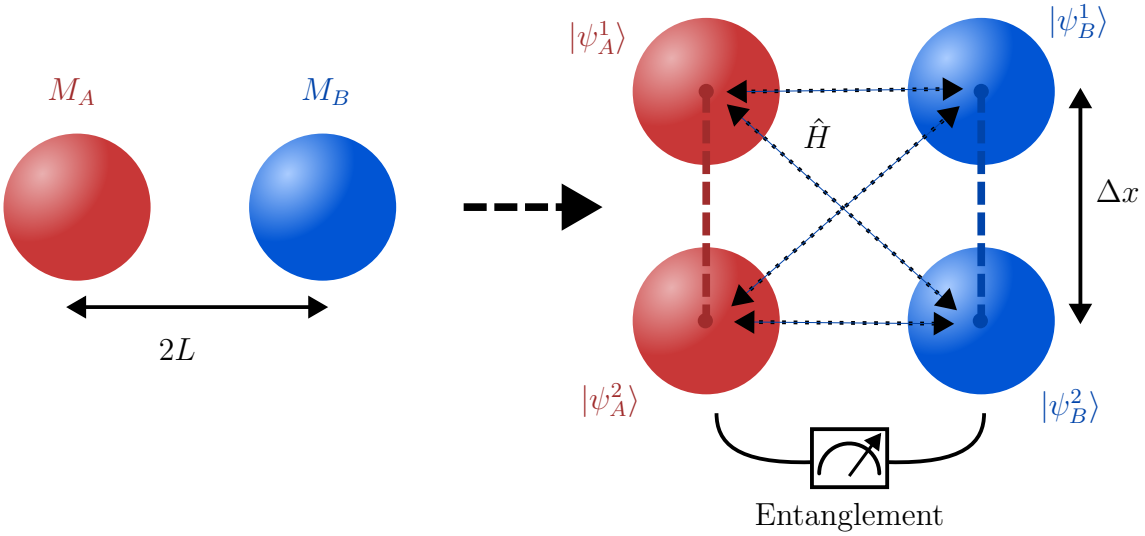

Figure 2.1: Schematic figure of the proposed experiment with two masses prepared in a spatial superposition state. The gravitational interaction $\hat{H}$ induces different phases to each of the superpositions due to the different distances between all masses. This results in measurable entanglement after some time evolution.

suspended and prepared in a coherent quantum superposition Schrödinger-cat-like state with a separation of Δx. Their center of masses are located a distance $2L$ away from each other. For now, a setup is chosen as in fig. 2.1, where the superposition locations are aligned parallel to each other. With the notation introduced in fig. 2.1, the initial state at $t = 0$ is given by

$$|\psi(t=0)\rangle = \frac{1}{2}\left(\left|\psi_A^1\right\rangle + \left|\psi_A^2\right\rangle\right) \otimes \left(\left|\psi_B^1\right\rangle + \left|\psi_B^2\right\rangle\right). \tag{2.1}$$

2.1 The Hamiltonian

The masses are assumed to interact only through their gravitational potential between each other. Any global factor of perturbation like the interaction with earth's gravitational field can be neglected. These kind of interactions manifests themselves only in a global phase factor for the evolved state. For now, all other local interactions like Casimir-Polder [2] or Coulomb forces are reduced to a minimum and are not considered at this stage.

The particles are assumed to be held in place by e.g. an optical trap and movement due to the gravitational acceleration is ignored on the time scales of the experiment. The Hamiltonian therefore only needs to include the gravitational interaction [1], i.e.

$$\hat{H} = \hat{V} = -\frac{GM_AM_B}{\left|\hat{D}\right|}, \tag{2.2}$$

where $\hat{D}$ is the distance operator between the masses depended on the individual positions $\hat{x_A}$ and $\hat{x_B}$.

During time evolution, the different superposition states build up different phases due to their different positions. I am interested whether this phase build-up results in measurable entanglement. This can, of cause, only happen if gravity is able to mediate entanglement.

2.2 Time evolution under a gravitational potential

The time evolution for a constant Hamiltonian $\hat{H} = \hat{V}(\hat{x}_i) = \text{const.}$ is governed by the Schrödinger equation

$$i\hbar\frac{\partial}{\partial t}|\psi(t)\rangle = \hat{H}|\psi(t)\rangle \tag{2.3}$$

with the general solution

$$|\psi(t)\rangle = e^{-i\hat{V}t/\hbar}|\psi(t=0)\rangle. \tag{2.4}$$

[1] In the low energy limit assumed here, relativistic effects do not play a role and the gravitational interaction between masses can be described by the classical Newtonian potential with the distance D between masses replaced by an operator $\hat{D}$.

By expressing $\hat{V}$ and ψ in the eigenbasis of the Hamiltonian like $\hat{V}\left|n\right\rangle = V_n\left|n\right\rangle$ and $\left|\psi(t=0)\right\rangle = \sum c_n\left|\psi_n\right\rangle$, the time evolution is given in the very simple form

$$\left|\psi(t)\right\rangle = \sum_n e^{-iV_n t/\hbar} c_n \left|\psi_n\right\rangle . \tag{2.5}$$

Expressed in the $\{\left|\psi_A^1\right\rangle, \left|\psi_A^2\right\rangle\} \otimes \{\left|\psi_B^1\right\rangle, \left|\psi_B^2\right\rangle\}$ basis, the time evolution of the system in (2.1) described by the Hamiltonian from eq. (2.2) is thus given by

$$\left|\psi(t)\right\rangle = \frac{1}{2}\Big(e^{i\phi_{11}}\left|\psi_A^1\right\rangle\left|\psi_B^1\right\rangle + e^{i\phi_{12}}\left|\psi_A^1\right\rangle\left|\psi_B^2\right\rangle + e^{i\phi_{21}}\left|\psi_A^2\right\rangle\left|\psi_B^1\right\rangle + e^{i\phi_{22}}\left|\psi_A^2\right\rangle\left|\psi_B^2\right\rangle\Big), \tag{2.6}$$

where the $\otimes$ symbol between the states was omitted. Here, the phases ϕ_{ij}, $i,j \in \{1,2\}$ are

$$\phi_{11} = \phi_{22} = \frac{GM_AM_B}{2\hbar L}t \qquad \text{and} \qquad \phi_{12} = \phi_{21} = \frac{GM_AM_B}{\hbar\sqrt{4L^2+(\Delta x)^2}}t. \tag{2.7}$$

Expanding the phases $\phi_{12} = \phi_{21} \approx GM_AM_B/\hbar\,[1/(2L) - (\Delta x)^2/(16L^3)] \equiv \phi_{11} - \Delta\phi$ a global phase ϕ_{12} can be factorized in eq. (2.6) as

$$\left|\psi(t)\right\rangle = \frac{1}{\sqrt{2}}e^{i\phi_{11}}\left[\left|\psi_A^1\right\rangle \otimes \frac{\left|\psi_B^1\right\rangle + e^{-i\Delta\phi}\left|\psi_B^2\right\rangle}{\sqrt{2}} + \left|\psi_A^2\right\rangle \otimes \frac{e^{-i\Delta\phi}\left|\psi_B^1\right\rangle + \left|\psi_B^2\right\rangle}{\sqrt{2}}\right]. \tag{2.8}$$

The density matrix of this state expressed in the natural basis for the system is given by

$$\rho(t) = \frac{1}{4}\begin{pmatrix} 1 & e^{i\Delta\phi} & e^{i\Delta\phi} & 1 \\ e^{-i\Delta\phi} & 1 & 1 & e^{-i\Delta\phi} \\ e^{-i\Delta\phi} & 1 & 1 & e^{-i\Delta\phi} \\ 1 & e^{i\Delta\phi} & e^{i\Delta\phi} & 1 \end{pmatrix}. \tag{2.9}$$

This state is entangled, if it cannot be represented in a product state $\left|\psi\right\rangle \neq \left|\psi_A\right\rangle \otimes \left|\psi_B\right\rangle$. Thus it is easy to see, that this condition is true if the two states multiplied by $\left|\psi_A^i\right\rangle$ not represent the same state i.e. they should not differ only by a phase factor. The evolved state is therefore entangled, if $\Delta\phi \neq k\pi$ with integer $k \in \mathbb{Z}$.

2.3 Fidelity of quantum states

In general, to compare the distance between two quantum states ρ and σ ("how similar they are") the ***fidelity*** $F(\rho,\sigma)$ is used. It is defined as [3, p. 409-412]

$$F(\rho,\sigma) = \operatorname{tr}\sqrt{\sqrt{\rho}\sigma\sqrt{\rho}} \tag{2.10}$$

and can be used as a distance measurement between quantum states. It is monotonic, concave and bounded between 0 and 1. If both states are equal $\rho = \sigma$, it is clear that

$F(\rho,\sigma)=1$, by using $\sqrt{\rho}\rho\sqrt{\rho}=\rho^2$. If both states commute, i.e. they are diagonalizable in the same orthogonal basis $\{|i\rangle\}$,

$$\rho=\sum_i r_i\,|i\rangle\langle i|\,;\quad \sigma=\sum_i s_i\,|i\rangle\langle i|\,,$$

the fidelity is given by [3, p. 409]

$$F(\rho,\sigma)=\operatorname{tr}\sqrt{\sum_i r_i s_i\,|i\rangle\langle i|}=\sum_i\sqrt{r_i s_i}.$$

This can be seen immediately by the use of the spectral theorem $\operatorname{tr}\sqrt{\rho}=\operatorname{tr}\Big\{U\sqrt{\operatorname{diag}(r_i)}U^\dagger\Big\}=\operatorname{tr}\operatorname{diag}(\sqrt{r_i})$. Another special case is given for the fidelity of a pure state $\rho=|\psi\rangle\langle\psi|$ and an arbitrary state σ [3, p. 409]:

$$F(|\psi\rangle\,,\sigma)=\operatorname{tr}\sqrt{\langle\psi|\,\sigma\,|\psi\rangle\,|\psi\rangle\langle\psi|}=\sqrt{\langle\psi|\,\sigma\,|\psi\rangle}.$$

If the state $\sigma=|\phi\rangle\langle\phi|$ is also pure, the fidelity reduces to

$$F(|\psi\rangle\,,|\phi\rangle)=|\langle\psi|\phi\rangle|\leq 1,$$

with equality being attained if the states are the same and only differ by a phase.

To quantify exactly how much the state $\psi(t)$ is entangled, a more sophisticated measurement for entanglement is necessary. In the next section, such a measurement - the ***logarithmic negativity*** - is discussed and calculated for the present system.

2.4 Entanglement measures

To check whether an arbitrary bipartite state ρ is entangled or not is no easy task. In fact, this problem is known to be NP-hard [4]. In a mathematical context, entanglement can be understood as the ***non-separability*** of a state $\rho_{AB}\in\mathcal{H}_A\otimes\mathcal{H}_B$ into two subsystems $\rho_A\in\mathcal{H}_A$ and $\rho_B\in\mathcal{H}_B$.

Lemma 2.1. *The trace norm $\|A\|_1\equiv\operatorname{tr}\sqrt{A^\dagger A}$ of a hermitian matrix A is equal to the sum of the absolute eigenvalues of A.*

Proof. This can be immediately seen by the spectral theorem:

$$\operatorname{tr}\sqrt{A^\dagger A}=\operatorname{tr}\sqrt{A^2}=\operatorname{tr}\Big\{U\sqrt{\operatorname{diag}(\lambda_1,\dots)^2}U^\dagger\Big\}=\sum_i\sqrt{\lambda_i^2}=\sum_i|\lambda_i|\,.$$

□

Proposition 2.1. *The **negativity** $\mathcal{N}(\rho)$ of a state ρ (defined below) is given as the absolute sum of all negative eigenvalues of ρ:*

$$\mathcal{N}(\rho) \equiv \frac{\left\|\rho^{\Gamma_A}\right\|_1 - 1}{2} = \left|\sum_{\lambda_i<0} \lambda_i\right|. \tag{2.11}$$

Proof. The proof is in parts given by Vidal [5]. It is known that the density matrix is hermitian: $\rho = \rho^\dagger$. Using lemma 2.1, the trace norm of the density matrix is is given as $\|\rho\|_1 = \sum \lambda_i = \operatorname{tr} \rho = 1$. The partial transpose ρ^{Γ_A} obviously also satisfies $\operatorname{tr} \rho^{\Gamma_A} = 1$ but might have negative eigenvalues. Since ρ^{Γ_A} is still hermitian, the trace norm is given by

$$\left\|\rho^{\Gamma_A}\right\|_1 = \sum_i |\lambda_i| = \sum_{\lambda_i \geq 0} \lambda_i + \sum_{\lambda_i<0} |\lambda_i| = \sum_i \lambda_i + 2 \sum_{\lambda_i<0} |\lambda_i| = 1 + 2 \sum_{\lambda_i<0} |\lambda_i|,$$

where in the last step $\sum \lambda_i = \operatorname{tr} \rho^{\Gamma_A} = 1$ was used. The negativity can be defined as $\mathcal{N}(\rho) = \left|\sum_{\lambda_i<0} \lambda_i\right|$ and the statement is shown. □

Remark. The method presented in proposition 2.1 is numerically more simple and requires zero matrix multiplications than to compute the sum of the square roots of the eigenvalues of $\rho^{\Gamma_A \dagger} \rho^{\Gamma_A}$ like shown in lemma 2.1. Furthermore in practice, ρ^{Γ_A} has at most only one negative eigenvalue and numeric stability is increased by only taking a single value instead of summing over all eigenvalues.

Remark. The ***logarithmic negativity*** [6] relates to the negativity as follows

$$E_N(\rho) = \log_2 \left\|\rho^{\Gamma_A}\right\|_1 = \log_2 \left(2\mathcal{N}(\rho) + 1\right) \tag{2.12}$$

and can therefore be easily calculated by using the above proposition 2.1. In comparison to the negativity, logarithmic negativity has additive properties [7]:

$$E_N(\rho \otimes \sigma) = E_N(\rho) + E_N(\sigma)$$

2.5 Issues with the experimental procedure

2.6 Entanglement measures

Why are they needed, what can one do?

Logarithmic negativity, properties, calculation

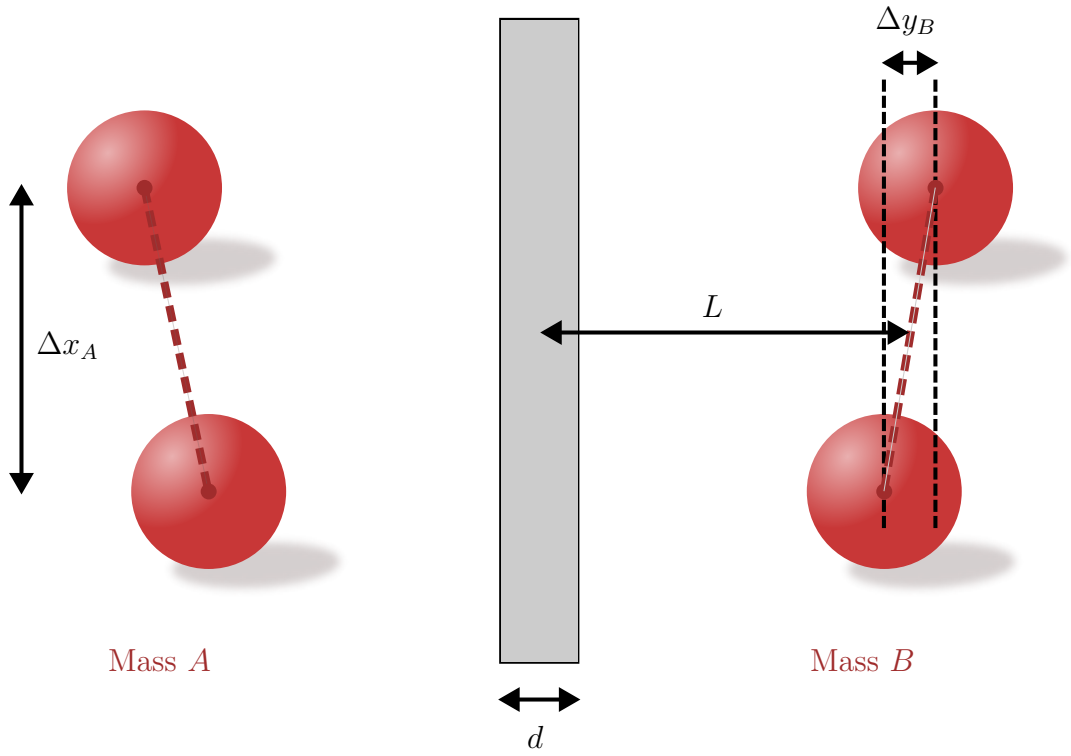

Figure 2.2: My problem

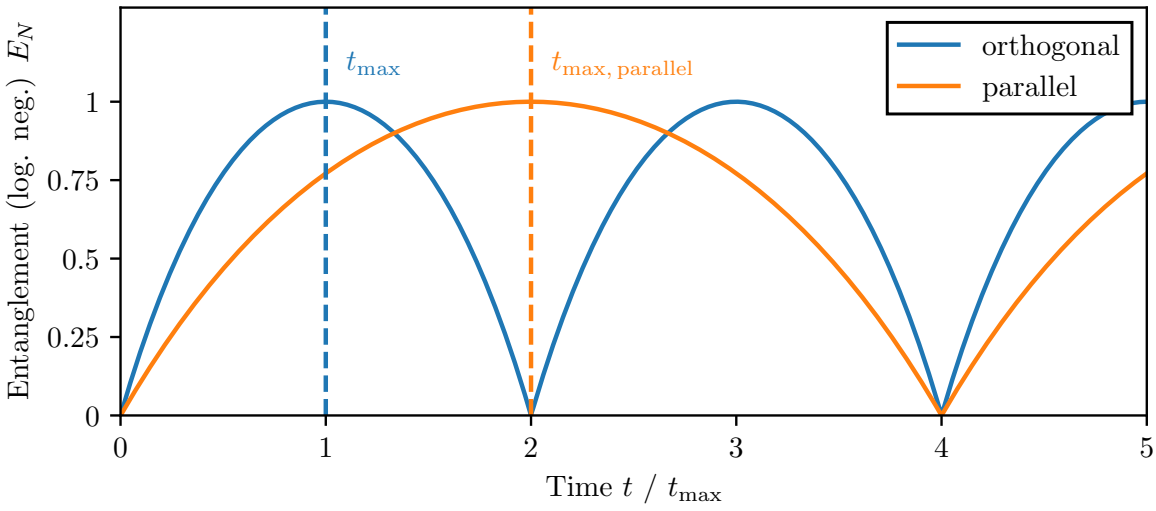

Figure 2.3: Entanglement dynamics quantified by the logarithmic negativity for two different orientations of the spatial superpositions relative to each other. The time of maximum entanglement $t_{\max}$ for the parallel configuration is given by $t_{\max} = 8\pi\hbar L^3/(GM_AM_Bd^2) \simeq 258\,\text{ms}$.

3 Casimir effect

General introduction and comparison with retarded van der Waals forces

$$F_{\text{Casimir}} = -\frac{\hbar c \pi^2}{240 L^4} A \tag{3.1}$$

$$V_{\text{Casimir}} = \frac{\hbar c \pi^2}{720 L^3} A \tag{3.2}$$

Lifshitz:

$$F_{\text{DD}} = \frac{\hbar c \pi^2}{240 L^4} \left(\frac{\varepsilon_r - 1}{\varepsilon_r + 1} \right)^2 \varphi(\varepsilon_r) \tag{3.3}$$

$$F_{\text{DM}} = \frac{\hbar c \pi^2}{240 L^4} \frac{\varepsilon_r - 1}{\varepsilon_r + 1} \varphi(\varepsilon_r) \tag{3.4}$$

The numeric function φ is shown in fig. 3.1.

3.1 Proximity force approximation

The Casimir-Polder force cannot be calculated easily for different shapes. There even exists no analytic expression for the simple (and for this thesis relevant) plate-sphere geometry for all ratios L/R and plate-sphere separations. For a general shape, even the sign of the force, i.e. whether it is attractive or repulsive, is often unknown. Fortunately, approximation methods exist and in particular the ***proximity-force-approximation (PFA)*** can be calculated very easily [8–10]. The PFA is only valid for small separations ($L/R \approx 1$) between the considered smooth bodies. The idea of this approximation is to divide the surfaces of the two bodies into infinitesimal small parallel plates with area $\mathrm{d}A$ and summing over the forces $\mathrm{d}F$ (or the Casimir-energy $\mathrm{d}E$) between them (see fig. 3.2):

$$E_{\text{PFA}} = \iint_A \mathrm{d}A \, \frac{E_{\text{plate-plate}}}{A} \tag{3.5}$$

where for the casimir energy per unit area $E_{\text{plate-plate}}/A$ either eq. (3.2) or any of the Lifshitz equations (3.3), (3.4) can be chosen. For the following calculations, it is important to distinguish between the distance between the plates center and the spheres center L (like used before) and the edge-to-edge distance $\mathscr{L} = L - R$.

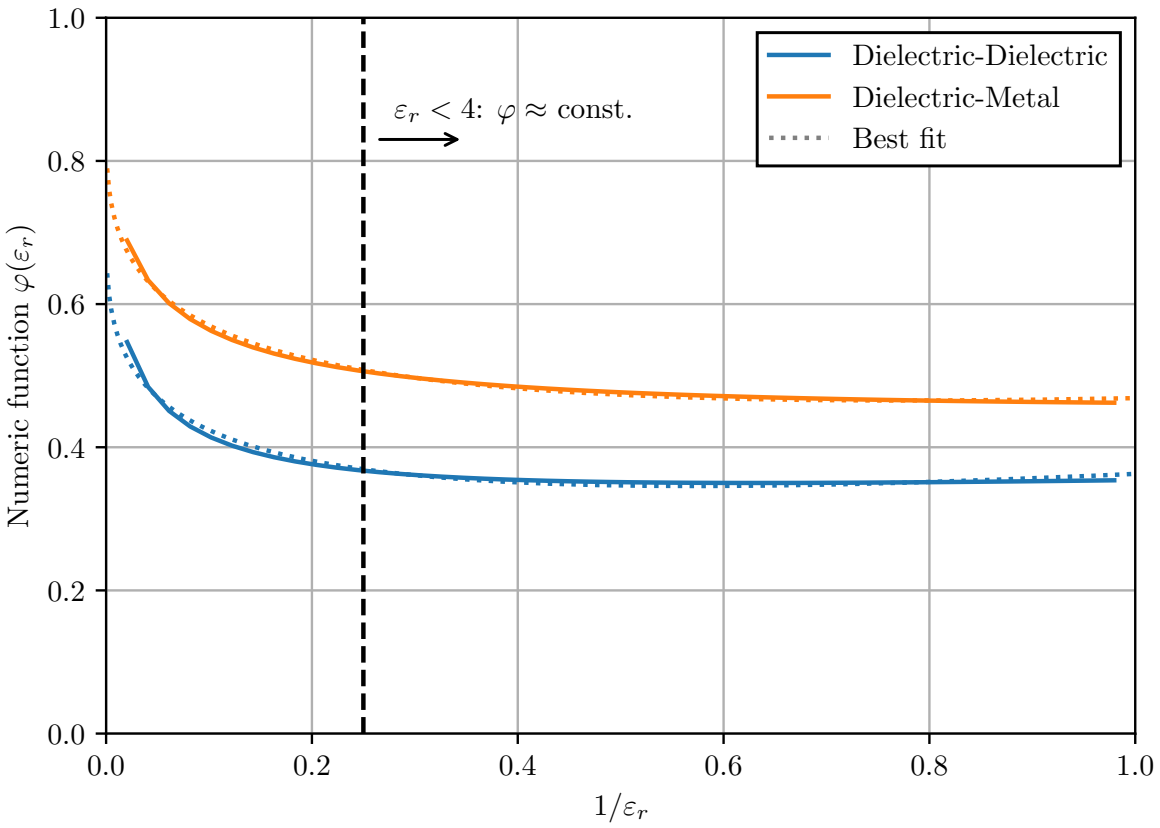

Figure 3.1: Numeric casimir interaction $\varphi(\epsilon_r)$ between **(blue)** two dielectric plates and **(orange)** a dielectric and a conductor.

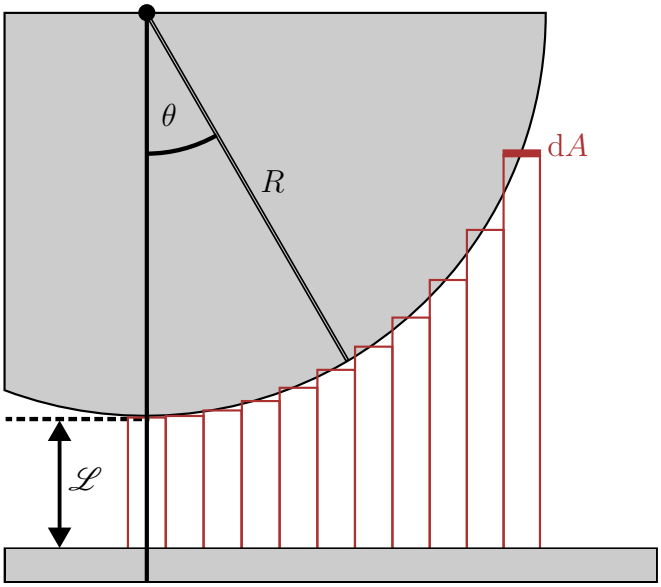

Figure 3.2: In the proximity force approximation the sphere is divided into infinitesimal plane areas $\mathrm{d}A$ which all exert a force $\mathrm{d}F$ according to eq. (3.1). All the contributions are added up together.

The problem with this approximation is, that it is ambiguous, what surface the area element $\mathrm{d}A$ represents. For the plate-sphere geometry, the element can be either chosen tangential to the sphere or parallel to the plate (or in theory any other fictitious surface somewhere in between) [10]. For the plate-sphere geometry, in the limit of the validity of the PFA $\mathscr{L} \ll R$ both methods yield the same result. For the following calculations, I choose $\mathrm{d}A$ parallel to the plate and the area can be parameterized with $r \in [0, R]$ and $\varphi \in [0, 2\pi]$ resulting in a distance z between the infinitesimal area elements $z(r) = \mathscr{L} + R - \sqrt{R^2 - r^2}$ [2]. The PFA eq. (3.5) then yields for a dielectric sphere against a perfectly conducting plate

$$E_{\text{plate-sphere}} = -\frac{\hbar c \pi^2}{720}\left(\frac{\varepsilon_r - 1}{\varepsilon_r + 1}\right)\varphi(\varepsilon_r)\int_0^R \mathrm{d}r \int_0^{2\pi} r\mathrm{d}\varphi \frac{1}{z(r)^3} \tag{3.6}$$

$$= -\frac{\hbar c \pi^3}{360}\left(\frac{\varepsilon_r - 1}{\varepsilon_r + 1}\right)\varphi(\varepsilon_r)\frac{R^2}{2\mathscr{L}^2(R + \mathscr{L})} \tag{3.7}$$

$$\approx -\frac{\hbar c \pi^3}{720}\left(\frac{\varepsilon_r - 1}{\varepsilon_r + 1}\right)\varphi(\varepsilon_r)\frac{R}{\mathscr{L}^2} \tag{3.8}$$

[2] Taking $\mathrm{d}A$ tangential to the sphere, it can be parameterized with $\theta \in [0, \pi/2]$ and $\varphi \in [0, 2\pi]$ resulting in $z(\theta) = \mathscr{L} + R - R\cos\theta$. The PFA eq. (3.5) yields with $\mathrm{d}A = R^2 \sin\theta \mathrm{d}\theta\mathrm{d}\varphi$ the result $\propto \frac{\pi R^2(R+2\mathscr{L})}{\mathscr{L}^2(R+\mathscr{L})^2}$ which in the limit of $\mathscr{L} \ll R$ results in the same expression as eq. (3.8).

3.2 Imperfect plate and spheres

Python numerical approach, gaussian modes (vibration modes of a spherical plane), perlin noise

3.3 Casimir forces between a conducting plate and a dielectric sphere

3.3.1 Polarizability of a dielectric sphere

The polarizability α is defined via

$$\mathbf{E}_\infty \alpha = \mathbf{p}, \tag{3.9}$$

where $\mathbf{p}$ is the induced dipole moment and $\mathbf{E}_\infty$ is the external electric field that induces the dipole moment. For a linear and uniform dielectric, it is given as $\mathbf{p} = \mathcal{V}\varepsilon_0(\varepsilon_r - 1)\mathbf{E}_{\text{in}}$ [11, p. 220-226]. Here, $\mathcal{V}$ is the volume of the object and $\mathbf{E}_{\text{in}}$ is the electric field inside the dielectric. The electrostatic boundary conditions for the problem are given by

$$V_{\text{in}}\Big|_{r=R} = V_{\text{out}}\Big|_{r=R} \quad \text{and} \quad \varepsilon_r\varepsilon_0 \frac{\partial V_{\text{in}}}{\partial r}\bigg|_{r=R} = \varepsilon_0 \frac{\partial V_{\text{out}}}{\partial r}\bigg|_{r=R} \tag{3.10}$$

and the electric potential outside of the sphere at $r \to \infty$ should be equal to the external dipole-inducing field $V_{\text{out}}|_{r\to\infty} = -\mathbf{E}_\infty \cdot \mathbf{r} = -E_\infty r\cos\theta$. The electric potential inside and outside the sphere can be calculated using the spherical decomposition of the general electric potential $V \propto 1/|\mathbf{r} - \mathbf{r}'|$ into Legendre Polynomials P_l [11, p. 188-190]:

$$V_{\text{in}}(r,\theta) = -E_\infty r\cos\theta + \sum_{l=0}^{\infty} A_l r^l P_l(\cos\theta), \tag{3.11}$$

$$V_{\text{out}}(r,\theta) = -E_\infty r\cos\theta + \sum_{l=0}^{\infty} \frac{B_l}{r^{l+1}} P_l(\cos\theta). \tag{3.12}$$

Applying both boundary conditions, it follows that [11, p. 249-251]

$$\begin{cases} A_l = B_l = 0 & \text{for } l \neq 1, \\ A_1 = -\frac{3}{\varepsilon_r+2}E_\infty, \quad B_1 = \frac{\varepsilon_r-1}{\varepsilon_r+2}R^3 E_\infty \end{cases} \tag{3.13}$$

and the resulting homogenous electric field $\mathbf{E}_{\text{in}} = -\nabla V_{\text{in}}$ inside the sphere is given as

$$\mathbf{E}_{\text{in}} = \frac{3}{\varepsilon_r + 2}\mathbf{E}_\infty. \tag{3.14}$$

The field is shown on the right in fig. 3.3.The polarizability α of the sphere can be now be determined to

$$\alpha_{\text{sphere}} = 4\pi\varepsilon_0 R^3 \left(\frac{\varepsilon_r - 1}{\varepsilon_r + 2}\right). \tag{3.15}$$

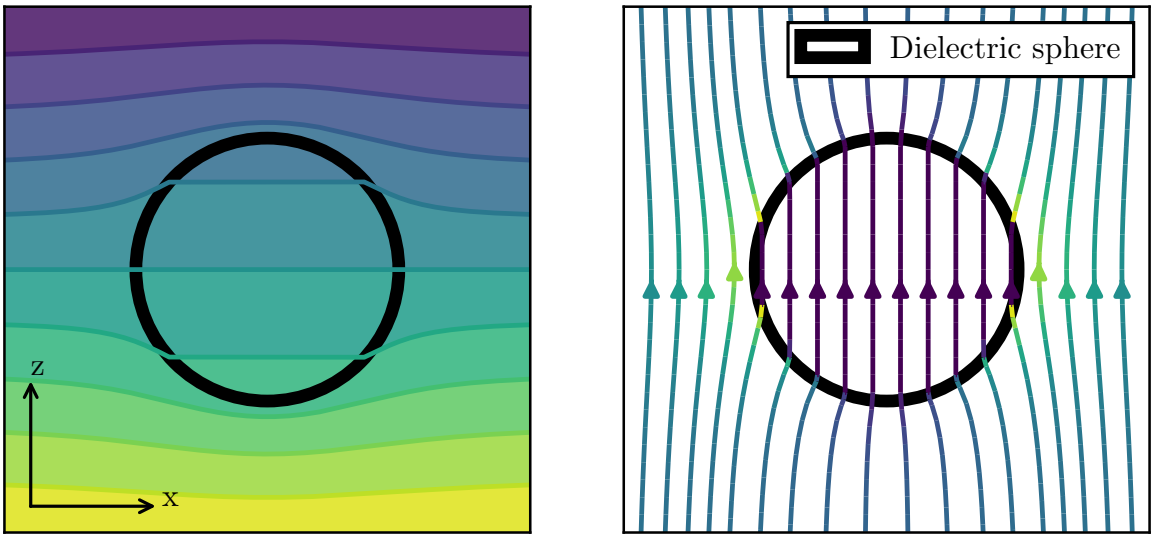

Figure 3.3: left: Electric potential V of a dielectric sphere in a external electric field $\mathbf{E}_\infty \parallel \mathbf{e_z}$. **right:** The corresponding electric field lines inside and outside the dielectric sphere.

4 The shield

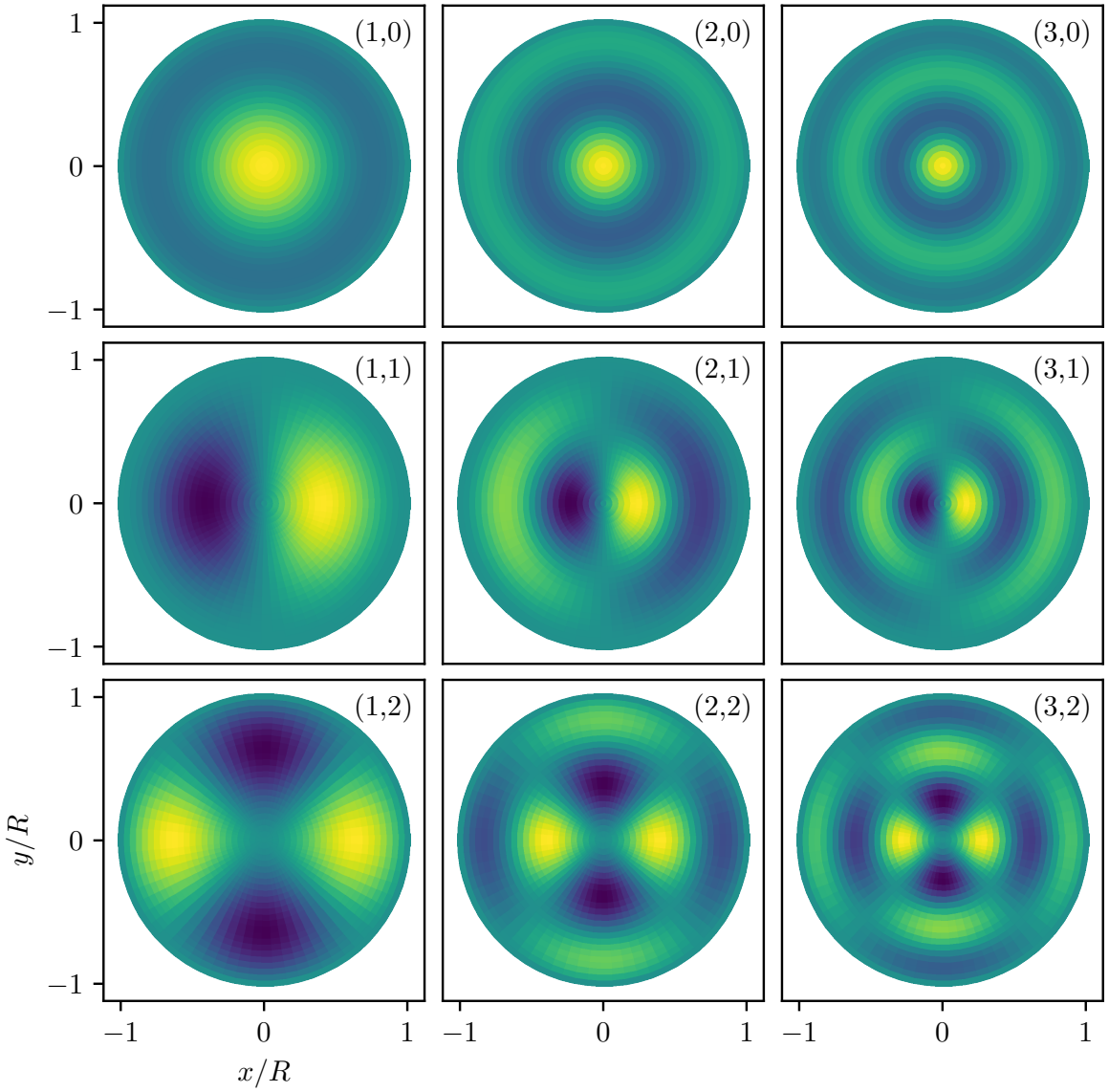

Figure 4.1: Vibrational modes of a spherical plate fixed at the edge with $R/d = 1000$.

5 The optimal setup

5.1 Orientation

E_N depending on the orientation:

$$E_N = \log_2 \left\{ 1 + \left| \sin\left(\frac{G M_A M_B t}{\hbar} \frac{\Delta x_A \Delta x_B}{8 L^3} \left[\sin\alpha \sin\beta - \frac{1}{2} \cos\alpha \cos\beta \right] \right) \right| \right\} \tag{5.1}$$

Time till the maximum entanglement ($E_N = 1$):

$$t_{\max} = \frac{8\pi L^3 \hbar}{2 G M_A M_B \Delta x_A \Delta x_B} \left| \sin\alpha \sin\beta - \frac{1}{2} \cos\alpha \cos\beta \right|^{-1} \tag{5.2}$$

with a global minimum for $\alpha, \beta \in [0, \pi]$ for the orthogonal orientation with $\alpha = \beta = \pi/2$. Here, the time till the maximum entanglement is given by

$$t_{\max} = \frac{4\pi \hbar L^3}{G M_A M_B \Delta x_A \Delta x_B} \simeq 129\,\mathrm{mn} \tag{5.3}$$

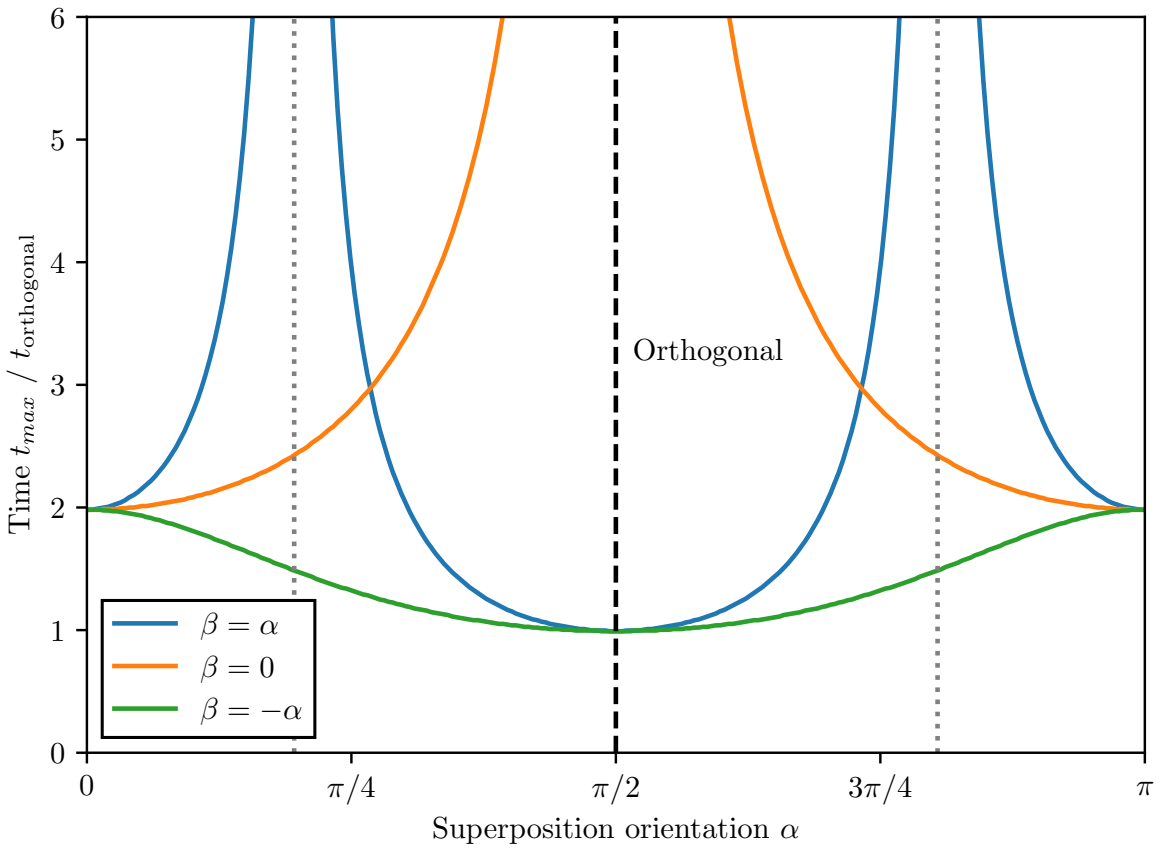
6
5
4
3
2
1
0
Time t_{max} / $t_{\text{orthogonal}}$
Orthogonal
$\beta = \alpha$
$\beta = 0$
$\beta = -\alpha$
0
$\pi/4$
$\pi/2$
$3\pi/4$
π
Superposition orientation α

Figure 5.1: ...

Bibliography

[1] S. Bose, A. Mazumdar, G. W. Morley, H. Ulbricht, M. Toroš, M. Paternostro, A. Geraci, P. Barker, M. S. Kim, and G. Milburn, "A Spin Entanglement Witness for Quantum Gravity", Phys. Rev. Lett. **119**, 240401 (2017) 10.1103/physrevlett.119.240401, arXiv:1707.06050.

[2] H. B. G. Casimir and D. Polder, "The Influence of Retardation on the London-van der Waals Forces", Physical Review **73**, 360–372 (1948) 10.1103/physrev.73.360.

[3] M. A. Nielsen and I. L. Chuang, ***Quantum computation and quantum information***, 10th anniversary ed. (Cambridge University Press, Cambridge, 2010), 1676 pages.

[4] L. Gurvits, "Classical deterministic complexity of Edmonds' problem and Quantum Entanglement", in Proceedings of the thirty-fifth annual acm symposium on theory of computing, Vol. 4, STOC03 (June 2003), pages 10–19, 10.1145/780542.780545, arXiv:quant-ph/0303055.

[5] G. Vidal and R. F. Werner, "A computable measure of entanglement", Phys. Rev. A **65**, 032314 (2001) 10.1103/physreva.65.032314, arXiv:quant-ph/0102117.

[6] M. Plenio, "Logarithmic negativity: a full entanglement monotone that is not convex.", Physical Review Letters **95**, 090503 (2005) 10.1103/PhysRevLett.95.090503, arXiv:quant-ph/0505071.

[7] M. B. Plenio and S. Virmani, "An introduction to entanglement measures", Quantum Information & Computation **7**, 1–51 (2005), arXiv:quant-ph/0504163.

[8] M. Hartmann, "Casimir effect in the plane-spheregeometry: Beyond the proximityforce approximation", PhD thesis (Universität Augsburg, July 2018).

[9] T. Emig, "Fluctuation induced quantum interactions between compact objects and a plane mirror", Journal of Statistical Mechanics: Theory and Experiment **2008**, P04007 (2007) 10.1088/1742-5468/2008/04/p04007, arXiv:0712.2199.

[10] A. Bulgac, P. Magierski, and A. Wirzba, "Scalar Casimir effect between Dirichlet spheres or a plate and a sphere", Physical Review D **73**, 025007 (2006) 10.1103/physrevd.73.025007.

[11] D. J. Griffiths, ***Elektrodynamik, Eine Einführung***, edited by U. Schollwöck, 4th edition (Pearson, Hallbergmoos, 2018), 1711 pages.

[12] J. S. Pedernales and M. B. Plenio, "On the origin of force sensitivity in tests of quantum gravity with delocalised mechanical systems", Contemporary Physics **64**, 147–163 (2023) 10.1080/00107514.2023.2286074, arXiv:2311.04745.

[13] A. Canaguier-Durand, R. Guérout, P. A. M. Neto, A. Lambrecht, and S. Reynaud, "The Casimir effect in the sphere-plane geometry", International Journal of Modern Physics Conference Series **14**, 250–259 (2012) 10.1142/s2010194512007374, arXiv:1202.3272.

[14] J. S. Pedernales, G. W. Morley, and M. B. Plenio, "Motional Dynamical Decoupling for Matter-Wave Interferometry", Phy. Rev. Lett. **125**, 023602 (2019) 10.1103/physrevlett.125.023602, arXiv:1906.00835.

[15] G. A. E. Vandenbosch, "The basic concepts determining electromagnetic shielding", American Journal of Physics **90**, 672–681 (2022) 10.1119/5.0087295.

[16] D. Carney, P. C. E. Stamp, and J. M. Taylor, "Tabletop experiments for quantum gravity: a user's manual", Classical and Quantum Gravity **36**, 034001 (2018) 10.1088/1361-6382/aaf9ca, arXiv:1807.11494.

[17] L. H. Ford, "Casimir Force between a Dielectric Sphere and a Wall: A Model for Amplification of Vacuum Fluctuations", Phys. Rev. A **58**, 4279–4286 (1998) 10.1103/physreva.58.4279, arXiv:quant-ph/9804055.

[18] T. W. van de Kamp, R. J. Marshman, S. Bose, and A. Mazumdar, "Quantum Gravity Witness via Entanglement of Masses: Casimir Screening", Phys. Rev. A **102**, 062807 (2020) 10.1103/physreva.102.062807, arXiv:2006.06931.

[19] I. G. Pirozhenko and M. Bordag, "On the Casimir repulsion in sphere-plate geometry", Physical Review D **87**, 085031 (2013) 10.1103/physrevd.87.085031, arXiv:1302.5290.

[20] T. Emig, N. Graham, R. L. Jaffe, and M. Kardar, "Casimir forces between arbitrary compact objects", Phys. Rev. Lett. **99**, 170403 (2007) 10.1103/physrevlett.99.170403, arXiv:0707.1862.

[21] E. M. Lifshitz, "The theory of molecular attractive forces between solids", Sov. Phys. JETP **2**, 73–83 (1956) 10.1016/b978-0-08-036364-6.50031-4.

A Proofs and other stuff